Research Square

Preprints are preliminary reports that have not undergone peer review.
They should not be considered conclusive, used to inform clinical practice,
or referenced by the media as validated information.

DNMT1-Induced miR-378a-3p Silencing Promotes Angiogenesis via NF-κB Signaling Pathway by Targeting TRAF1 in Hepatocellular Carcinoma

Bin Zhu
Affiliated Hospital of Nantong University
Jun-Jie Chen
Affiliated Hospital of Nantong University
Ying Feng
Affiliated Hospital of Nantong University
Jun-Ling Yang
Affiliated Hospital of Nantong University
Hua Huang
Affiliated Hospital of Nantong University
Chung WY
Leicester General Hospital
Yi-Lin Hu
Affiliated Hospital of Nantong University
Wan-Jiang Xue (xuewanjiang@ntu.edu.cn)
Affiliated Hospital of Nantong University https://orcid.org/0000-0002-0137-7331

Research Article

Keywords: Angiogenesis, HCC, miR-378a-3p, TRAF1, DNA methylation

Posted Date: June 4th, 2021

DOI: https://doi.org/10.21203/rs.3.rs-581090/v1

License: This work is licensed under a Creative Commons Attribution 4.0 International License.
Read Full License

Abstract

Background: Angiogenesis plays an important role in the occurrence, development and metastasis of hepatocellular carcinoma (HCC). miR-378a-3p participates in tumorigenesis and tumor metastasis according to previous studies, yet the exact role it plays in HCC angiogenesis remains poorly understood.

Methods: qRT-PCR was used to investigate the expression of miR-378a-3p in HCC tissues and cell lines. The effects of miR-378a-3p on HCC in *vitro* and in *vivo* were examined by CCK-8, transwell assay, tube formation and matrigel plug assay. RNA sequencing, bioinformatics analysis, luciferase reporter assay, immunofluorescence assay and ChIP assay were used to detected the molecular mechanism of miR-378a-3p-induced inhibition of angiogenesis.

Results: We confirmed that the expression of miR-378a-3p was significantly downregulated and was associated with microvascular density (MVD) in HCC, which indicated a short survival time of HCC patients, and reducing miR-378a-3p expression led to a significant increase in angiogenesis in *vitro* and in *vivo*. miR-378a-3p directly targeted TNF receptor associated factor 1 (TRAF1) to attenuate NF-κB signaling, and then decreases secreted vascular endothelial growth factor (VEGF). DNA methyltransferase 1 (DNMT1) mediated hypermethylation of miR-378a-3p was responsible for downregulating of miR-378a-3p. Moreover, a series of investigation indicated that p65 initiated a positive feedback loop, which could up-regulate DNMT1 to promote hypermethylation of the miR-133a-3p promoter.

Conclusion: Our study indicates that a novel DNMT1/miR-378a-3p/TRAF1/ NF-κB positive feedback loop in HCC cells, which may become a potential therapeutic target for HCC.

1. Background

Hepatocellular carcinoma (HCC) is one of the most common digestive tract tumors in the world, with approximately 850,000 new cases and at least 780,000 deaths annually[1]. With the advancements in diagnostic techniques and the development of surgical strategies, such as hepatectomy, liver transplantation, local ablation therapy, and transarterial chemoembolization, the survival rate and quality of life of HCC patients has significantly improved; however, the five-year survival rate is still less than 30% [2]. Angiogenesis is known to regulate tumor growth and metastasis by providing nutrients for tumor cells[3]. HCC is a typical angio-rich tumor characterized by abnormal angiogenesis. In clinical practice, multi-target tyrosine kinase inhibitors targeting vascular endothelial growth factor (VEGF) could inhibit the growth and development of HCC through suppressing the angiogenesis. However, these drugs is still limited[4–6]. Therefore, it is vital to explore new targets for the treatment of HCC via regulating HCC angiogenesis.

NF-κB signal transduction is a highly conserved signaling pathway, and its abnormal activation plays an important role in tumor occurrence and development. A previous study found that NF-κB had a wide range of transcription activity and multiple links to angiogenesis[7, 8]. It has been shown that inhibition of

NF-kB can eliminate the production of VEGF and angiogenesis in a variety of conditions[9]. Studies have indicated that NF-κB contributes to angiogenesis in prostate[10], breast[11], colorectal[12], and pancreatic cancers[13]. Meiotic recombination protein (REC8) has been shown to inhibit NF-κB/p65 activity and its downstream gene VEGF and ultimately exert anti-angiogenesis function in tumor angiogenesis in gastric cancer cells[14]. The expression of prenyl diphosphate synthase subunit 2 (PDSS2-DEL2) was found to be positively related to microvascular counts in HCC, and activation of the NF-κB pathway promoted metastasis and angiogenesis of HCC[15]. Therefore, inhibiting NF-kB activity, leading to the decreased tumor-induced blood vessels formation, might be an important strategy for the treatment of HCC.

MicroRNAs (miRNAs) are endogenous noncoding RNAs, approximately 22 nucleotides in length, and are known to regulate various biological processes, including angiogenesis and tumor progression[16, 17]. miRNA-378a, including miR-378a-3p and miR-378a-5p, is located on human chromosome 5q32 and owns abundant biological functions[18]. The expression of miR-378a is involved in the regulation of mitochondria, glucose metabolism, autophagy, and other metabolic pathways[19, 20]. Besides, miR-378a plays an active role in the occurrence and development of malignant tumors[21, 22]. The miR-378a-5p suppressed angiogenesis of oral squamous cell carcinoma by the regulation of Kallikrein-related peptidase 4 (KLK4). The miR-378a-3p could bind to the target genes, mitogen-activated protein kinase 1 (MAPK1) and growth factor receptor bound protein 2 (GRB2), and leads to the silence of their expression and reverses cisplatin resistance of ovarian cancer cells[23]. The overexpression of miR-378 also promotes the migration and invasion of human hepatoblastoma cells[24]. Pogribny et al. fed rats with the oncogenic agent tamoxifen to induce HCC. After 12 weeks and 24 weeks, miRNA expression profiles were studied in the liver of rats, and it was found that miR-378 expression was decreased in the tamoxifen-treated group[25]. However, the mechanism of the effects of miR-378a on the occurrence and development of HCC is still unclear.

In this study, we identified the novel function in miR-378a-3p that play an antitumor role in HCC angiogenesis and was correlated with a favorable prognosis. Further in vitro and in vivo experiments demonstrated that miR-378a-3p abolished the oncogenic function of NF-κB/p65 for silencing its targeted gene TNF receptor associated factor 1 (TRAF1), the activator of NF-κB. What's more, p65 promoted the transcriptional expression of DNA methyltransferase 1 (DNMT1) what could act as the DNA methyltransferase of miR-378a-3p. In total, the regulatory mechanism network of HCC angiogenesis formed a positive feedback loop via DNMT1/miR-378a-3p/TRAF1/ NF-κB.

2. Materials And Methods

2.1 Clinical samples

108 pairs of original HCC tissues and para-carcinoma tissues were oh2tained from patients undergoing surgery at the affiliated hospital of Nantong University h2etween 2004 and 2010. Another cohort of 10 matched fresh HCC cases was collected from the same hospital. All patients had not received chemotherapy, radiotherapy, or immunotherapy h2efore undergoing surgery. The follow-up was

completed in August 2015 (median follow-up 65 months; range, 2–95 months). The samples were collected promptly during surgical resection and stored at -80°C. The experimental protocol was approved h2y the ethics committee of the affiliated hospital of Nantong University. Also, written informed consent was oh2tained from all participants.

2.2 Cell lines and culture condition

MHCC-97H, MHCC-97L and HCCLM3 cells lines were donated h2y the Liver Cancer Institute, ZhongShan Hospital. LO2, SMMC-7721 and human umh2ilical vein endothelial cells (HUVECs) were procured from GeneChem (Shanghai, China). All cell lines were cultured in DMEM medium, supplemented with 10% fetal h2ovine serum (FH2S), ampicillin, and streptomycin in a 5% CO2 humidified chamh2er at 37°C.

2.3 Cell transfection and drug treatment

The sequences of the mimic or inhih2itors were designed and composed h2y GenePharma (Suzhou, China). Cell transfection was performed on a six-well plate using the Lipofectamine 3000 reagent (Invitrogen, USA). Cells were collected 48 h post-transfection to detect the expression. DNMT1 siRNA, DNMT3A siRNA, DNMT3H2 siRNA were oh2tained from GeneChem. The siRNA sequences are shown in Tah2le S1. For drug treatment, cells were treated with 10μM 5-Azacytidine (5-Aza, MedChemExpress, Shanghai, China) for 48 h, 50μg/ml SN50 (Solarh2io, H2eijing, China) for 24h, or 60μg/ml LPS (MedChemExpress) for 24h. All experiments were performed in triplicate.

2.4 qRT-PCR analysis

Total RNA was extracted using the Trizol reagent (Invitrogen). We performed qRT-PCR following a previously describh2ed method[26]. The h2ulge-loop RT primer and qPCR primers specific for has-miR-378a-3p and has-miR-378a-5p were designed and synthesized h2y Rih2oH2io (Guangzhou, China). Tah2le S2 lists the primers used in this study. All experiments were performed in triplicate.

2.5 Suh2cellular fractionation and Western h2lot assay

Suh2cellular fractionation was performed using a Nuclear and Cytoplasmic Protein Extraction Kit (Sangon H2iotech), in accordance with the manufracturer's instructions. Total protein separation and western h2lot were performed following a previously describh2ed method[27]. The following antih2odies were used: anti-NF-κH2 p65 (Proteintech; Wuhan, China; 66535-1-Ig), anti-p-IκH2α (Cell Signaling Technology; H2oston, USA, 14D4), anti-p-IKKβ (Ah2cam; Shanghai, China, ah259195), anti-β-actin (Proteintech; 66009-1-Ig), anti-lamin H21 (Proteintech; 66095-1-Ig), and anti-TRAF1 (Proteintech; 26845-1-AP). All experiments were performed in triplicate.

2.6 Immunohistochemistry (IHC)

IHC was performed following a previously describh2ed method[27]. The following antih2odies were used: anti-CD34 (Proteintech; 14486-1-AP), anti-VEGF (Proteintech; 19003-1-AP), Staining intensity was scored manually h2y two independent experienced pathologists as: 0 = no staining, 1 = weak staining, 2 = moderate staining, and 3 = strong staining. The percentage of positive cells was also assessed according

to four scores: 1 (0%-10%), 2 (11%-50%), 3 (51%-80%), and 4 (81%-100%). The final IHC score was calculated h2y multiplying the intensity score h2y the percentage of positive cells. Low expression of VEGF was for scores from 0 to 5. The ones with scores ≥ 6 were considered high expression[28]. CD34 antih2ody was used to stain vascular endothelial cells and then calculated microvessal density (MVD). The field of maximal CD34 expression was found in tumor tissues. Within this field, the area of maximal angiogenesis was selected, and microvessels were counted on a 200×magnification field. Low expression of MVD was for scores from 0 to 3. The ones with scores ≥ 4 were considered high MVD[29].

2.7 Immunofluorescence

Immunofluorescence was performed as describh2ed in our previous study[27]. The cells were incuh2ated overnight with anti-NF-κH2 p65 at 4℃, followed h2y washing thrice with PH2S. Next, the cells with fluorescent Alexa Fluor 594-conjugated goat anti-rah2h2it IgG (AH2clonal, Wuhan, China; AS039) and DyLight-488 goat anti-mouse IgG (MultiSciences; Hangzhou, China; GAM4882). Finally, nuclei were lah2eled with DAPI (Cell Signaling Technology) for 15 min, and the images of stained cells were captured h2y the H2X41 microscope (Olympus, Japan). All experiments were performed in triplicate.

2.8 Wound healing assay, Cell invasion assay, and Colony assay

We added 0.4-μm-thick pore inserts (Corning, USA) into 6-well culture plates. HUVECs (1×10^6 cells) were placed in the lower strata and treated HCCLM3 and SMMC-7721 cells were placed in the upper inserts and co-cultured in DMEM medium with 5% FH2S for 48 h. Next, we collected the treated HUVECs for wound healing assay, cell invasion assay, and colony assay. These experiments were performed as describh2ed previously[30]. All experiments were performed in triplicate.

2.9 Tuh2e formation assay

We added Matrigel (170 μL) to cold 48-well culture plates and allowed to solidify at 37°C for 30 min. Next, treated HUVECs (1×10^4 cells/well) were seeded onto the matrigel. After incuh2ation for 8 h at 37℃, the formation of polygonal tuh2es was assessed microscopically at 100x magnification. All experiments were performed in triplicate.

2.10 Matrigel plug assay

Male H2ALH2/C nude mice aged 6 weeks were purchased from the Animal Lah2oratory Center of Nantong University (Nantong, China). HCCLM3 and SMMC-7721 cells were treated with miR-378a-3p mimics or inhih2itors for 48 h, respectively. These cells resuspended in a serum-free medium (5×10^6 cells in 50μL) and then mixed with 400 μL of matrigel. The cell/Matrigel mixture was injected into nude mouse. 7 days later, the mice were sacrificed, and the matrix plug was removed for analysis. All animal experiments were approved h2y the Institutional Animal Care and Use Committee of Nantong University following current guidelines for animal care and welfare.

2.11 ELISA

HCC cells were seeded in 6-well plates and incuh2ated in serum-free medium for 24 hours. The conditioned medium was collected, and the concentration of VEGF was quantified using VEGF ELISA kits (Jianglaih2io, shanghai, China, JL18341) according to the manufacturer's instructions. All experiments were performed in triplicate.

2.12 Luciferase reporter assays

NF-κH2 luciferase assays were performed via the co-transfection with the pNF-κH2-luciferase plasmid (GeneChem), control luciferase plasmid, pRL-TK Renilla, miRNA mimics and miRNA mimics control into HCC cells h2y Lipofectamine 3000 (Invitrogen). The 3'-UTR sequences of TRAF1 containing miR-378a-3p h2inding sites were synthesized and constructed into the luciferase reporter vector (GeneChem). Next, SMMC-7721 and HCCLM3 cells transfected with miRNA mimics and control were co-transfected with the luciferase reporter vectors. The wild-type DNMT1 promoter and a promoter with mutated NF-κH2-h2inding sites were designed h2y GeneChem. DNMT1-WT or DNMT1-MUT was co-transfected with pcDNA3.1 vector or pcDNA3.1 p65 (GeneChem). After 48 h, the luciferase activity was measured with a dual-luciferase assay kit (H2eyotime, shanghai, China). The results are presented as the relative luciferase activity of Renilla, which was normalized to the activity of firefly luciferase. All experiments were performed in triplicate.

2.13 Chromatin immunoprecipitation (ChIP)

ChIP was done using a previously descrih2ed method[31]. ChIP assays were performed using a Pierce Magnetic ChIP Kit (Thermo Fisher Scientific, Waltham, MA, USA) according to the manufacturer's protocol. Anti-p65 antih2ody and normal IgG (MultiSciences) were used for immunoprecipitation. Primer sequences for ChIP assays were as follows: forward, 5'-TGTCACCATGCCCAGCAAAT-3'; reverse, 5'-TAAATTAAGAAGCACCATGT-3'. All experiments were performed in triplicate.

2.14 Online h2ioinformatics analysis

Two datasets, GSE108724 and GSE54751, were download from the Gene Expression Omnih2us (GEO) datah2ase to determine the differential miR-378a-3p expression. The University of California Santa Cruz (UCSC) Xena H2rowser was used to explore and analyze the genes in the TCGA datah2ase. Putative miR-378a-3p target genes were predicted h2y miRWalk (http://mirwalk.umm.uni-heidelh2erg.de/) and miRTarH2ase (http://mirtarh2ase.mh2c.nctu.edu.tw/). The GEPIA datah2ase (http://gepia2.cancer-pku.cn/) was used to analyse the expression correlation h2etween DNMT1 and p65. JASPAR (jaspar.genereg.net/) was used to predict the putative transcription factors of DNMT1. STRING dataset (https://string-dh2.org/) was used to predict the functional pathways correlated with TRAF1.

2.15 RNA sequencing

Three repeated pairs of SMMC-7721/miR-378a-3p mimic and control groups were prepared for RNA sequencing, which was performed h2y GENEWIZ (Soochow, China). A significant difference in mRNA expression (*P*-value < 0.05 and |log2 FC| >1) h2etween groups was identified using the fold change cut-off.

2.16 Statistical analysis

The measured data were represented as the mean ± SD. Student's t-test was used for statistical comparisons h2etween experimental groups. The correlations h2etween miR-378a-3p expression and various clinicopathological factors were performed using chi-squared test. The Cox regression model was used to evaluated prognostic factors. Logistic regression analysis was performed to identify risk factors affecting miR-378a-3p levels in HCC. The proh2ah2ility of differences in overall survival (OS) and disease-free survival (DFS) were assessed with Kaplan-Meier and log-rank tests. Spearman's correlation rank analysis was used to analyse categorical variah2les. All statistical analyses were performed with SPSS v24.0 software. P < 0.05 was considered as statistically significant.

3. Results

3.1 miR-378a-3p expression is downregulated in HCC patients and correlated with HCC angiogenesis

To elucidate the functional roles of miR-378a in HCC, we found that miR-378a levels were down-regulated in HCC tissues compared to normal tissues from The Cancer Genome Atlas (TCGA) and GSE54751 datasets (Fig. 1A, B). Next, we compared the mRNA levels of the two strands of miR-378a, miR-378a-3p and miR-378a-5p, in 10 matched fresh HCC and corresponding normal tissues, respectively. The miR-378a-3p and miR-378a-5p expression was significantly downregulated in HCC, and miR-378a-3p showed a substantially higher difference (Fig. 1C, D). The GSE108724 dataset and 108 matched samples also confirmed that miR-378a-3p was downregulated in HCC (Fig. 1E, F). Combined with the clinical data of 108 patients, we found that the decreased miR-378a-3p expression was closely associated with tumor thrombus and MVD (Table 1). Moreover, multiple logistic regression analysis showed expression miR-378a-3p was significantly inversely correlated with MVD (p < 0.001, odds ratio [OR] = 0.070, 95% confidence interval [CI]: 0.027–0.179). The results was also validated in 10 paired HCC and normal tissues via FISH assay for miR-378a-3p and IHC for MVD (Fig. 1G, H). Kaplan-Meier analysis showed that HCC patients with lower miR-378a-3p expression had worse OS and DFS rates than those with higher miR-378a-3p expression (Fig. 1I, J). Also, the results of Cox multivariate regression analysis revealed that miR-378a-3p was an independent, effective prognostic factor (Table 2).

3.2 miR-378a-3p inhibited HCC angiogenesis in vitro and in vivo

To further study the function of miR-378a-3p in HCC angiogenesis, HUVECs growth, metastasis experiments and tube formation were investigated. Real-time PCR (qRT-PCR) was performed to investigate the expression of miR-378a-3p in four HCC cell lines and human normal liver cell line LO2. The expression of miR-378a-3p in HCC cell lines was significantly lower than those in LO2 cells (Fig. 2A). Then, we established miR-378a-3p-overexpressing HCC cells with LM3 and miR-378a-3p-knockdowning HCC cells with SMMC-7721 (Fig. 2B). A co-culture system was used to culture treated HCC cells along with HUVECs for 48h (Fig. 2C). Reduced proliferation was observed in HUVECs co-cultured with higher miR-378a-3p expression HCC cells (Fig. 2D, E, Supplementary Fig. S1A). Wound healing assay and Matrigel assay indicated that the migration and invasion ability of HUVECs was decreased after co-culturing with the miR-378a-3p-overexpressing HCC cells, while anti-miR-378a-3p resulted in the elevated (Fig. 2F, G, Supplementary Fig. S1B). The supernatant from miR-378a-3p-overexpressing HCC cells inhibited HUVECs tube formation (Fig. 2H). Correspondingly, these results were confirmed by the *in vivo* experiments. The matrigel plug assay was used to analyze the potential of neovascularization to further identify the antitumor function of miR-378a-3p in HCC. The matrigel plugs collected from the NC group had more blood vessels (Fig. 2I). The results of IHC showed that the MVD (Fig. 2J) and the expression of VEGF (Fig. 2K) was lower in the miR-378a-3p-overexpression group than in the NC group. The result of ELISA indicted that the secretion of VEGF was downregulated by miR-378a-3p mimics and upregulated by miR-378a-3p inhibitor in conditioned medium of HCC cell lines (Fig. 2L). Thus, our data suggested that miR-378a-3p negatively regulated HCC angiogenesis in vitro and in vivo.

3.3 TRAF1 acted as a direct target gene of miR-378a-3p in HCC cells

RNA sequencing was performed to understand the molecular mechanism of miR-378a-3p-induced inhibition of angiogenesis in SMCC-7721 cells. We identified 297 differentially expressed genes (DEGs), including 133 upregulated DEGs and 164 downregulated DEGs (Fig. 3A). Next, we used the online bioinformatics tool miRWalk and miRTarbase to predict the potential target of miR-378a-3p. Combined with the results of gene microarray analysis, TRAF1 was the only putative target of miR-378a-3p and was downregulated while the miR-378a-3p was upregulated in SMCC-7721 cells (Fig. 3B). Furthermore, we used a bioinformatics database to examine whether miR-378a-3p could bind to TRAF1. We found that TRAF1 had a potential binding site of miR-378a-3p, and then we inserted the wild-type or mutant TRAF1 into a luciferase reporter vector (Fig. 3C). Transfection of miR-378a-3p mimic significantly inhibited the luciferase activity of the wild-type TRAF1 reporter, and this effect was completely eradicated for the mutant reporter (Fig. 3D). Additionally, miR-378a-3p mimics downregulated the mRNA and protein expressions of TRAF1, while miR-378a-3p inhibitor upregulated the TRAF1 expression in HCC cells (Fig. 3E, F). Thus, these results indicated that TRAF1 acted as a direct target of miR-378a-3p in HCC.

3.4 The miR-378a-3p inhibited the activation of the NF-κB signaling pathway by downregulating TRAF1 expression

To identify the molecular mechanism by which miR-378a-3p inhibits HCC angiogenesis. STRING dataset was used to predict the top 10 functional pathways correlated with TRAF1 (Fig. 4A). As we and others have shown that TRAF1 activated NF-κB signaling pathway and promoted cancer development[32]. Next, we performed luciferase reporter assays to determine the function of miR-378a-3p in NF-κB signaling activation and found that the relative luciferase activity of NF-κB was reduced in miR-378a-3p-overexpressing cells (Fig. 4B) and was increased in miR-378a-3p knockdown cells (Fig. 4C). Meanwhile, the results of immunofluorescence assays shown that the nuclear expression of p65 was decreased in miR-378a-3p-overexpressing cells (Fig. 4D) while increased in miR-378a-3p knockdown cells (Fig. 4E). The results of western blot showed that the overexpression of miR-378a-3p inhibited the phosphorylation of IκBα and IKK-β while miR-378a-3p knockdown increased their phosphorylation. Additionally, the upregulated expression of miR-378a-3p reduced nuclear p65 expression, whereas knockdown of miR-378a-3p increased nuclear p65 expression (Fig. 4F, G). To further characterise the antioncogenic function of miR-378a-3p in HCC, we compared the cells transfected with miR-378a-3p NC, mimics, and mimics combined with lipopolysaccharide (LPS), which activates the NF-κB pathway, LPS reversed the proliferation, migration, invasion and angiogenesis abilities inhibitions of miR-378a-3p and the results were also confirmed by the transfection of miR-378a-3p inhibitor and SN50, which inhibits the NF-κB pathway (Supplementary Fig. S2A-E). ELISA also demonstrated that the secretion of VEGF in conditioned medium of HCC cell lines was upregulated by miR-378a-3p mimics and LPS than miR-378a-3p mimics alone, while the cells transfected with miR-378a-3p inhibitor and treated with SN50 exhibited lower secretion of VEGF (Supplementary Fig. S2F). Next, western blot confirmed that LPS attenuated the inhibiting effect of miR-378a-3p mimics and SN50 repressed the promoting effect of miR-378a-3p inhibitor (Supplementary Fig. S3A, B). Together, our data suggested that miR-378a-3p inhibited HCC angiogenesis by suppressing the activation of the NF-κB signaling pathway.

3.5 miR-378a-3p is hypermethylated by DNMT1 and silenced in HCC tissues and cells

The methylation of the promoter DNA could reduce the miRNA expression[33, 34]. We treated SMMC-7721 and HCCLM3 cells with a demethylating agent, 5-Aza-CdR, to confirm whether the decrease in miR-378a-3p in HCC was caused by DNA methylation. As expected, the expression of miR-378a-3p was dramatically increased after treatment with 5-Aza-CdR (Fig. 5A). Because the miR-378a-3p promoter is hypermethylated in HCC, we hypothesized that the deregulation of a specific methylase or demethylase induces this process. To clarify the potential roles of the various DNMTs in mediating miR-378a-3p promoter methylation in HCC, we knocked down DNMT1, DNA methyltransferase 3 alpha (DNMT3A), and DNA methyltransferase 3 beta (DNMT3B) in HCC cells using specific small interfering RNAs (siRNAs) (Fig. 5B). The relative miR-378a-3p mRNA level of HCC cells transfected with DNMT1, but not those with

DNMT3A and DNMT3B was obviously increased (Fig. 5C). Moreover, overexpression of DNMT1 significantly suppressed miR-378a-3p expression (Fig. 5D). To further test this speculation, we evaluated the expression level of DNMT1 in HCC patients with GEPIA database (Fig. 5E). We also examined the expression level of DNMT1 in 10 pairs of clinical HCC and normal tissues. The results revealed that DNMT1 was generally expressed at a higher level in HCC tissues (Fig. 5F). Spearman's rank correlation analysis revealed a negative correlation between DNMT1 and miR-378a-3p expression (Fig. 5G). The above results suggested that DNMT1 could directly induce the hypermethylation of miR-378a-3p and downregulate its expression.

3.6 p65 promoted DNMT1 transcription and induced miR-378a-3p silencing mediated by DNA hypermethylation

Consistent with our results, silencing miR-378a-3p can activate p65, which is a well-known transcription factor and involved in tumor genesis and development[35]. Interestingly, the results indicated p65-overexpression increased DNMT1 expression and reduced the expression of miR-378a-3p in HCC cells (Fig. 6A, B). Based on this phenomenon, we assumed that p65 could feedback regulate the expression of DNMT1. that GEPIA database showed that p65 was positively correlated to DNMT1 in HCC (Fig. 6C). To elucidate the mechanisms underlying p65 induced upregulation of DNMT1, we analyzed the DNMT1 promoter and identified a potential binding sites for p65 (Fig. 6D) and then constructed vectors containing wildtype or mutant promoters of DNMT1 for luciferase reporter assay (Fig. 6E). We found that the transfection of p65 significantly enhanced the luciferase activity of the DNMT1 WT reporter, whereas this effect was completely reversed by the mutant reporter, indicating that this site was the key region of p65 mediated DNMT1 upregulation (Fig. 6F). The results of the ChIP assay determined that p65 directly bound to the DNMT1 promoter in HCC cells (Fig. 6G). Thus, these results suggested that silencing of miR-378a-3p mediated by DNA methylation facilitated angiogenesis of HCC through up-regulating the expression of p65, which positively provided feedback for the methylation of miR-378a-3p (Fig. 6H).

4. Discussion

Angiogenesis plays pivotal roles in tumor progression and metastasis. Thus, it is important to investigate the role of miR-378a-3p in regulating HCC angiogenesis to develop therapeutic interventions. Several studies have shown that miR-378a-3p plays different functions in different tumors[23, 36–40]. In this study, we found that the expression of miR-378a-3p was downregulated in HCC and was related to the poor prognosis. The expression of miR-378a-3p had a significant effect on angiogenesis by a series of experiments in vitro and in vivo. Consistent with these experiments, the results of GO analysis in RNA sequencing showed enrichment of "negative regulation of endothelial cell proliferation" and "negative regulation of endothelial cell differentiation" (Supplementary Fig. S4A). Thus, we confirmed that miR-378a-3p plays a new antiangiogenic role in HCC and provides promising means for HCC treatment.

TRAF1, a member of the TRAF family, is known to regulate the cascade of typical and atypical NF-κB signaling. Compared with the other members, TRAF1 has received more attention due to its lack of RING and zinc finger structures[41]. The upregulated anti-apoptotic protein TRAF1 activates the PI3K/Akt/NF-κB signaling pathway in non-small cell lung cancer (NSCLC)[42]. TRAF1 is necessary for the development of UV radiation-induced skin cancer, and the deletion of TRAF1 in mice has been shown to significantly inhibit the formation of skin tumors[43]. Also, miR-483 has been shown to inhibit the proliferation and migration of colorectal cancer cells by targeting TRAF1[44]. Studies have shown that miR-127-5p alleviates severe pneumonia by targeting TRAF1 to inactivate Akt and NF-κB signaling pathways[45]. In our study, TRAF1 was confirmed as the downstream regulator of miR-378a-3p. Also, miR-378a-3p could negatively regulate the expression of TRAF1. These data further suggested that miR-378a-3p was inversely correlated with the TRAF1 in HCC.

DNA methylation is one of the most important epigenetic modifications and is involved in various human diseases[46]. DNA methyltransferases (DNMTs) are a vital epigenetic family of enzymes that catalyze and maintain DNA methylation. Studies have identified three types of DNMTs with specific biological functions: DNMT1, DNMT3A, and DNMT3B. Compared with DNMT3A and DNMT3B, DNMT1 plays a more vital biological roles[47]. Numerous studies have found that DNMT1 is associated with abnormal DNA methylation, and elevated expression of DNMT1 has been shown to promote the occurrence and development of cancers of the esophagus, breast, pancreas, thyroid, and colon[48]. Enhancer of Zeste Homolog 2 (EZH2) has been shown to recruit DNMT1 to methylate the CpG island of the miR-484 promoter, which negatively regulates the Wnt/MAPK and TNF signaling pathways by upregulating the expression of HNF1A and MMP14, respectively, to inhibit the growth and metastasis of cervical cancer[49]. Jiang et al. found that ARID2 inhibited epithelial-mesenchymal transition (EMT) of HCC cells by recruiting DNMT1 to the Snail promoter region, inducing promoter methylation and inhibiting Snail transcription[50]. Our results provide a new mechanism indicating DNMT1-induced regulation of the downregulated expression of miR-378a-3p.

The expression of DNMT1 is regulated by multiple factors. A histone H3 peptide ubiquitinated (H3Ub) stimulates the maintenance activity of DNMT1 by increasing its methylation processivity. The SET and RING finger-associated domain (SRA) domain of ubiquitin like with PHD and ring finger domains 1 (Uhrf1) additively stimulates DNMT1 activity with H3Ub peptides[51]. Deletion of lysine-specific histone demethylase 1 (LSD1) induces the loss of DNA methylation. This loss correlates with a decrease in DNMT1 protein, as a result of reduced DNMT1 stability. DNMT1 protein is methylated in vivo, and its methylation is enhanced in the absence of LSD1[52]. Multiple transcription factors including E2F1 and SP1 mediate the transcriptional activation of DNMT1 by the activated MEK/ERK pathway[53]. In lung cancer, p65 is known to directly recruit DNMT1 to chromatin to enhance the methylation of the BRMS1 promoter; thus, acting as a transcriptional suppressor[54]. Therefore, we hypothesized that p65 induced DNMT1 transcription by promoting the activation of the promoter of DNMT1 in HCC. The DNMT1 promoter region was analyzed by JASPAR, and the region contains a hypothesized binding site of p65. Additionally, we found that DNMT1 was positively correlated to p65 in GEPIA. Combined with ChIP assay and dual-luciferase reporter assay, these experiments indicated that p65 promoted DNMT1 transcription.

Conclusion

In conclusion, our study unravels that miR-378a-3p is a potential predictor and therapeutic target for the treatment of HCC. Low miR-378a-3p expression was associated with MVD and poor survival outcome in HCC patients. DNA hypermethylation-induced silencing of miR-378a-3p facilitates HCC angiogenesis by up-regulating TRAF1 and NF-κB signaling. As a transcriptional coactivator, p65 promotes DNMT1 expression, which positively regulates miR-378a-3p promoter methylation.

Abbreviations

HCC: Hepatocellular carcinoma; MVD: Microvascular density; HUVECs: Human umbilical vein endothelial cells; TRAF1: TNF receptor associated factor 1; VEGF: Vascular endothelial growth factor; DNMT1: DNA methyltransferase 1; PDSS2-DEL2: Prenyl diphosphate synthase subunit 2; KLK4: Kallikrein-related peptidase 4; MAPK1: Mitogen-activated protein kinase 1; GRB2: Growth factor receptor bound protein 2; FBS: Fetal bovine serum; NSCLC: Non-small cell lung cancer; qRT-PCR: Quantitative reverse; transcriptase polymerase chain reaction; EZH2: Enhancer of Zeste Homolog 2; EMT: Epithelial-mesenchymal transition; H3Ub: H3 peptide ubiquitinated; SRA: SET and RING finger-associated; Uhrf1: ubiquitin like with PHD and ring finger domains 1; LSD1: Lysine-specific histone demethylase 1.

Declarations

Ethics Approval and Consent to Participate

In animal experiments, we comply with the ARRIVE guidelines, the UK Animals (Scientific Procedures) Act, 1986 and associated guidelines, EU Directive 2010/63/EU for animal experiments, or the National Institutes of Health guide for the care and use of Laboratory animals (NIH Publications No. 8023, revised 1978). The mice purchased are male. In addition, animal experiments were performed using protocols approved by the Animal Center of the Medical College of Nantong University.

Consent for publication

Not applicable.

Availability of data and materials

The datasets used or analysed during the current study are available from the corresponding author on reasonable request

Competing interests

The authors confirm that there are no conflicts of interest.

Funding

This work was supported by the National Natural Science Foundation of China (81672409), the Foundation of Nantong science and technology bureau (MSZ19204), and the Foundation of Nantong science and technology bureau (MS12019026).

Authors' Contributions

WJX and YLH wrote the original manuscript and analyzed the data. BZ, JJC, YF, JLY, HH and CWY performed the experiments and analyzed the data. All authors read and approved the final manuscript.

Acknowledgements

We thank the Liver Cancer Institute of ZhongShan Hospital (Shanghai, China) for the gift of the MHCC-97L, MHCC-97H and HCCLM3 cell lines. Thanks to the Research center of clinical medicine of Hospital of Nantong University for providing us with the precise laboratory equipment needed for this subject.

References

1. Lee SE, Alcedo KP, Kim HJ, Snider NT. Alternative Splicing in Hepatocellular Carcinoma. Cell Mol Gastroenterol Hepatol. 2020;10:699–712.
2. Llovet JM, Zucman-Rossi J, Pikarsky E, Sangro B, Schwartz M, Sherman M, et al. Hepatocellular carcinoma. Nat Rev Dis Primers. 2016;2:16018.
3. Alsaab HO, Al-Hibs AS, Alzhrani R, Alrabighi KK, Alqathama A, Alwithenani A, et al. Nanomaterials for Antiangiogenic Therapies for Cancer: A Promising Tool for Personalized Medicine. *Int J Mol Sci* 2021; 22.
4. Sbenati RM, Zaraei SO, El-Gamal MI, Anbar HS, Tarazi H, Zoghbor MM, et al. Design, synthesis, biological evaluation, and modeling studies of novel conformationally-restricted analogues of sorafenib as selective kinase-inhibitory antiproliferative agents against hepatocellular carcinoma cells. Eur J Med Chem. 2021;210:113081.
5. Eso Y. Targeting Angiogenesis for Advanced Hepatocellular Carcinoma. Intern Med. 2021;60:321–2.
6. Zhu XD, Tang ZY, Sun HC. Targeting angiogenesis for liver cancer: Past, present, and future. Genes Dis. 2020;7:328–35.
7. Zhou W, Yang L, Nie L, Lin H. Unraveling the molecular mechanisms between inflammation and tumor angiogenesis. Am J Cancer Res. 2021;11:301–17.
8. Tang X, Cao T, Zhu Y, Zhang L, Chen J, Liu T, et al. PIM2 promotes hepatocellular carcinoma tumorigenesis and progression through activating NF-kappaB signaling pathway. Cell Death Dis. 2020;11:510.
9. Xia Y, Shen S, Verma IM. NF-kappaB, an active player in human cancers. Cancer Immunol Res. 2014;2:823–30.
10. Mu HQ, He YH, Wang SB, Yang S, Wang YJ, Nan CJ, et al. MiR-130b/TNF-alpha/NF-kappaB/VEGFA loop inhibits prostate cancer angiogenesis. Clin Transl Oncol. 2020;22:111–21.

11. Liang S, Chen Z, Jiang G, Zhou Y, Liu Q, Su Q, et al. Activation of GPER suppresses migration and angiogenesis of triple negative breast cancer via inhibition of NF-kappaB/IL-6 signals. Cancer Lett. 2017;386:12–23.
12. Wang R, Ma Y, Zhan S, Zhang G, Cao L, Zhang X, et al. B7-H3 promotes colorectal cancer angiogenesis through activating the NF-kappaB pathway to induce VEGFA expression. Cell Death Dis. 2020;11:55.
13. Azoitei N, Becher A, Steinestel K, Rouhi A, Diepold K, Genze F, et al. PKM2 promotes tumor angiogenesis by regulating HIF-1alpha through NF-kappaB activation. Mol Cancer. 2016;15:3.
14. Liu M, Xu W, Su M, Fan P. REC8 suppresses tumor angiogenesis by inhibition of NF-kappaB-mediated vascular endothelial growth factor expression in gastric cancer cells. Biol Res. 2020;53:41.
15. Zeng T, Tang Z, Liang L, Suo D, Li L, Li J, et al. PDSS2-Del2, a new variant of PDSS2, promotes tumor cell metastasis and angiogenesis in hepatocellular carcinoma via activating NF-kappaB. Mol Oncol. 2020;14:3184–97.
16. Annese T, Tamma R, De Giorgis M, Ribatti D. microRNAs Biogenesis, Functions and Role in Tumor Angiogenesis. Front Oncol. 2020;10:581007.
17. Gallach S, Calabuig-Farinas S, Jantus-Lewintre E, Camps C. MicroRNAs: promising new antiangiogenic targets in cancer. *Biomed Res Int* 2014; 2014: 878450.
18. Machado IF, Teodoro JS, Palmeira CM, Rolo AP. miR-378a: a new emerging microRNA in metabolism. Cell Mol Life Sci. 2020;77:1947–58.
19. Zhang T, Shi H, Liu N, Tian J, Zhao X, Steer CJ, et al. Activation of microRNA-378a-3p biogenesis promotes hepatic secretion of VLDL and hyperlipidemia by modulating ApoB100-Sortilin1 axis. Theranostics. 2020;10:3952–66.
20. Krist B, Podkalicka P, Mucha O, Mendel M, Sepiol A, Rusiecka OM, et al. miR-378a influences vascularization in skeletal muscles. Cardiovasc Res. 2020;116:1386–97.
21. Fu H, Zhang J, Pan T, Ai S, Tang L, Wang F. miR378a enhances the sensitivity of liver cancer to sorafenib by targeting VEGFR, PDGFRbeta and cRaf. Mol Med Rep. 2018;17:4581–8.
22. Tanaka H, Hazama S, Iida M, Tsunedomi R, Takenouchi H, Nakajima M, et al. miR-125b-1 and miR-378a are predictive biomarkers for the efficacy of vaccine treatment against colorectal cancer. Cancer Sci. 2017;108:2229–38.
23. Xu ZH, Yao TZ, Liu W. miR-378a-3p sensitizes ovarian cancer cells to cisplatin through targeting MAPK1/GRB2. Biomed Pharmacother. 2018;107:1410–7.
24. Ma J, Lin J, Qian J, Qian W, Yin J, Yang B, et al. MiR-378 promotes the migration of liver cancer cells by down-regulating Fus expression. Cell Physiol Biochem. 2014;34:2266–74.
25. Pogribny IP. MicroRNA dysregulation during chemical carcinogenesis. Epigenomics. 2009;1:281–90.
26. Hu YL, Feng Y, Ma P, Wang F, Huang H, Guo YB, et al. HAX-1 promotes the migration and invasion of hepatocellular carcinoma cells through the induction of epithelial-mesenchymal transition via the NF-kappaB pathway. Exp Cell Res. 2019;381:66–76.

27. Liu JZ, Hu YL, Feng Y, Guo YB, Liu YF, Yang JL, et al. Rafoxanide promotes apoptosis and autophagy of gastric cancer cells by suppressing PI3K /Akt/mTOR pathway. Exp Cell Res. 2019;385:111691.
28. Zhu J, Huang S, Wu G, Huang C, Li X, Chen Z, et al. Lysyl Oxidase Is Predictive of Unfavorable Outcomes and Essential for Regulation of Vascular Endothelial Growth Factor in Hepatocellular Carcinoma. Dig Dis Sci. 2015;60:3019–31.
29. Mazzanti R, Messerini L, Comin CE, Fedeli L, Ganne-Carrie N, Beaugrand M. Liver angiogenesis as a risk factor for hepatocellular carcinoma development in hepatitis C virus cirrhotic patients. World J Gastroenterol. 2007;13:5009–14.
30. Qu F, Zhu B, Hu YL, Mao QS, Feng Y. LncRNA HOXA-AS3 promotes gastric cancer progression by regulating miR-29a-3p/LTbetaR and activating NF-kappaB signaling. Cancer Cell Int. 2021;21:118.
31. Hu YL, Feng Y, Chen YY, Liu JZ, Su Y, Li P, et al. SNHG16/miR-605-3p/TRAF6/NF-kappaB feedback loop regulates hepatocellular carcinoma metastasis. J Cell Mol Med. 2020;24:7637–51.
32. Guo F, Sun A, Wang W, He J, Hou J, Zhou P, et al. TRAF1 is involved in the classical NF-kappaB activation and CD30-induced alternative activity in Hodgkin's lymphoma cells. Mol Immunol. 2009;46:2441–8.
33. Shi W, Tang T, Li X, Deng S, Li R, Wang Y, et al. Methylation-mediated silencing of miR-133a-3p promotes breast cancer cell migration and stemness via miR-133a-3p/MAML1/DNMT3A positive feedback loop. J Exp Clin Cancer Res. 2019;38:429.
34. Zeng B, Zhang X, Zhao J, Wei Z, Zhu H, Fu M, et al. The role of DNMT1/hsa-miR-124-3p/BCAT1 pathway in regulating growth and invasion of esophageal squamous cell carcinoma. BMC Cancer. 2019;19:609.
35. Mori Y, Akita K, Tanida S, Ishida A, Toda M, Inoue M, et al. MUC1 protein induces urokinase-type plasminogen activator (uPA) by forming a complex with NF-kappaB p65 transcription factor and binding to the uPA promoter, leading to enhanced invasiveness of cancer cells. J Biol Chem. 2014;289:35193–204.
36. Ding N, Sun X, Wang T, Huang L, Wen J, Zhou Y. miR378a3p exerts tumor suppressive function on the tumorigenesis of esophageal squamous cell carcinoma by targeting Rab10. Int J Mol Med. 2018;42:381–91.
37. Song X, Ning W, Niu J, Zhang G, Liu H, Zhou L. CBX8 acts as an independent RNA-binding protein to regulate the maturation of miR-378a-3p in colon cancer cells. Hum Cell. 2021;34:515–29.
38. Zhang Y, Yu R, Li L. LINC00641 hinders the progression of cervical cancer by targeting miR-378a-3p/CPEB3. J Gene Med. 2020;22:e3212.
39. Tupone MG, D'Aguanno S, Di Martile M, Valentini E, Desideri M, Trisciuoglio D, et al. microRNA-378a-5p iS a novel positive regulator of melanoma progression. Oncogenesis. 2020;9:22.
40. Niu F, Dzikiewicz-Krawczyk A, Koerts J, de Jong D, Wijenberg L, Fernandez Hernandez M, et al. MiR-378a-3p Is Critical for Burkitt Lymphoma Cell Growth. *Cancers (Basel)* 2020; 12.
41. Zapata JM, Reed JC. TRAF1: lord without a RING. *Sci STKE* 2002; 2002: pe27.

42. Song L, Xiong H, Li J, Liao W, Wang L, Wu J, et al. Sphingosine kinase-1 enhances resistance to apoptosis through activation of PI3K/Akt/NF-kappaB pathway in human non-small cell lung cancer. Clin Cancer Res. 2011;17:1839–49.
43. Yamamoto H, Ryu J, Min E, Oi N, Bai R, Zykova TA, et al. TRAF1 Is Critical for DMBA/Solar UVR-Induced Skin Carcinogenesis. J Invest Dermatol. 2017;137:1322–32.
44. Niu ZY, Li WL, Jiang DL, Li YS, Xie XJ. Mir-483 inhibits colon cancer cell proliferation and migration by targeting TRAF1. Kaohsiung J Med Sci. 2018;34:479–86.
45. Chen C, Lin S, Zhou L, Wang J, Chen J, Yu R, et al. MicroRNA-127-5p attenuates severe pneumonia via tumor necrosis factor receptor-associated factor 1. Exp Ther Med. 2020;20:2856–62.
46. Kulis M, Esteller M. DNA methylation and cancer. Adv Genet. 2010;70:27–56.
47. Ren W, Gao L, Song J. Structural Basis of DNMT1 and DNMT3A-Mediated DNA Methylation. *Genes (Basel)* 2018; 9.
48. Xu X, Nie J, Lu L, Du C, Meng F, Song D. LINC00337 promotes tumor angiogenesis in colorectal cancer by recruiting DNMT1, which suppresses the expression of CNN1. *Cancer Gene Ther* 2020.
49. Hu Y, Wu F, Liu Y, Zhao Q, Tang H. DNMT1 recruited by EZH2-mediated silencing of miR-484 contributes to the malignancy of cervical cancer cells through MMP14 and HNF1A. Clin Epigenetics. 2019;11:186.
50. Jiang H, Cao HJ, Ma N, Bao WD, Wang JJ, Chen TW, et al. Chromatin remodeling factor ARID2 suppresses hepatocellular carcinoma metastasis via DNMT1-Snail axis. Proc Natl Acad Sci U S A. 2020;117:4770–80.
51. Mishima Y, Brueckner L, Takahashi S, Kawakami T, Otani J, Shinohara A, et al. Enhanced processivity of Dnmt1 by monoubiquitinated histone H3. Genes Cells. 2020;25:22–32.
52. Wang J, Hevi S, Kurash JK, Lei H, Gay F, Bajko J, et al. The lysine demethylase LSD1 (KDM1) is required for maintenance of global DNA methylation. Nat Genet. 2009;41:125–9.
53. Li J, Wang R, Hu X, Gao Y, Wang Z, Li J, et al. Activated MEK/ERK Pathway Drives Widespread and Coordinated Overexpression of UHRF1 and DNMT1 in Cancer cells. Sci Rep. 2019;9:907.
54. Liu Y, Mayo MW, Nagji AS, Smith PW, Ramsey CS, Li D, et al. Phosphorylation of RelA/p65 promotes DNMT-1 recruitment to chromatin and represses transcription of the tumor metastasis suppressor gene BRMS1. Oncogene. 2012;31:1143–54.

Tables

Table 1. Relationships between *miR-378a-3p* expression and clinicopathological characteristics of HCC patients

Clinicopathological characteristics	n	Low expression	High expression	*P* value
Total	108	54	54	
Gender				0.060
Male	75	33	42	
Female	33	21	12	
Age (years)				0.440
≤60	83	41	42	
>60	25	13	12	
Grade of differentiation				0.123
Low	56	32	24	
High-Middle	52	22	30	
Tumor diameter (cm)				0.123
≤5	50	29	21	
>5	58	25	33	
Liver function (Child-Pugh stage)				0.588
A	92	45	47	
B or C	16	9	7	
Hepatocirrhosis				0.288
Absent	31	13	18	
Present	77	41	36	
HBV infection				0.555
Absent	43	20	23	
Present	65	34	31	
Tumor thrombus				0.011
Absent	65	26	39	
Present	43	28	15	
AFP (ng/ml)				0.083
≤20	53	22	31	
>20	55	32	23	

BCLC stage				0.552
A	41	19	22	
B, C, or D	67	35	32	
Envelope				0.700
Absent	52	25	27	
Present	56	29	27	
Tumor satellite				0.079
Absent	63	27	36	
Present	45	27	18	
MVD				<0.001
High	59	45	14	
Low	49	9	40	

*P<0.05. AFP: serum alpha fetoprotein; HBV: hepatitis B virus; BCLC: Barcelona Clinic Liver Cancer.

Table 2. Univariate and multivariable analyses of OS and DFS in HCC patients

Variable	OS			DFS		
	Univariate analysis	Multivariable analysis		Univariate analysis	Multivariable analysis	
	P>|z|	*P*>|z|	HR(95%CI)	*P*>|z|	*P*>|z|	HR(95%CI)
miR-378a-3p expression						
Low (n=54) vs. high (n=54)	<0.001	0.003	0.414(0.232-0.736)	0.001	0.010	0.454(0.249-0.828)
Gender						
Male (n=75) vs. female (n=33)	0.944			0.737		
Age (years)						
≤60 (n=83) vs. >60 (n=25)	0.518			0.837		
Grade of differentiation						
Low (n=56) vs. middle-high (n=52)	0.330			0.444		
Tumor diameter (cm)						
≤5 (n=50) vs. >5 (n=58)	0.588			0.294		
Liver function (Child-Pugh stage)						
A (n=92) vs. B or C (n=16)	0.901			0.980		
Hepatocirrhosis						
Absent (n=31) vs. present (n=77)	0.874			0.698		
Hepatitis B virus						
Absent (n=43) vs. present (n=65)	0.189			0.692		
Tumor thrombus						
Absent (n=65) vs. present (n=43)	0.079			0.052		
AFP (ng/ml)						
≤20 (n=53) vs.	0.264			0.973		

>20 (n=55)						
BCLC stage						
I (n=41) vs. II, III, or IV (n=67)	0.194			0.149		
Envelope						
Absent (n=52) vs. present (n=56)	0.142			0.946		
Tumor satellite						
Absent (n=63) vs. present (n=45)	0.146			0.411		
MVD						
High (n=59) vs. Low (n=49)	<0.001	0.018	2.048(1.129-3.715)	0.001	0.022	2.036(1.106-3.746)

Figures

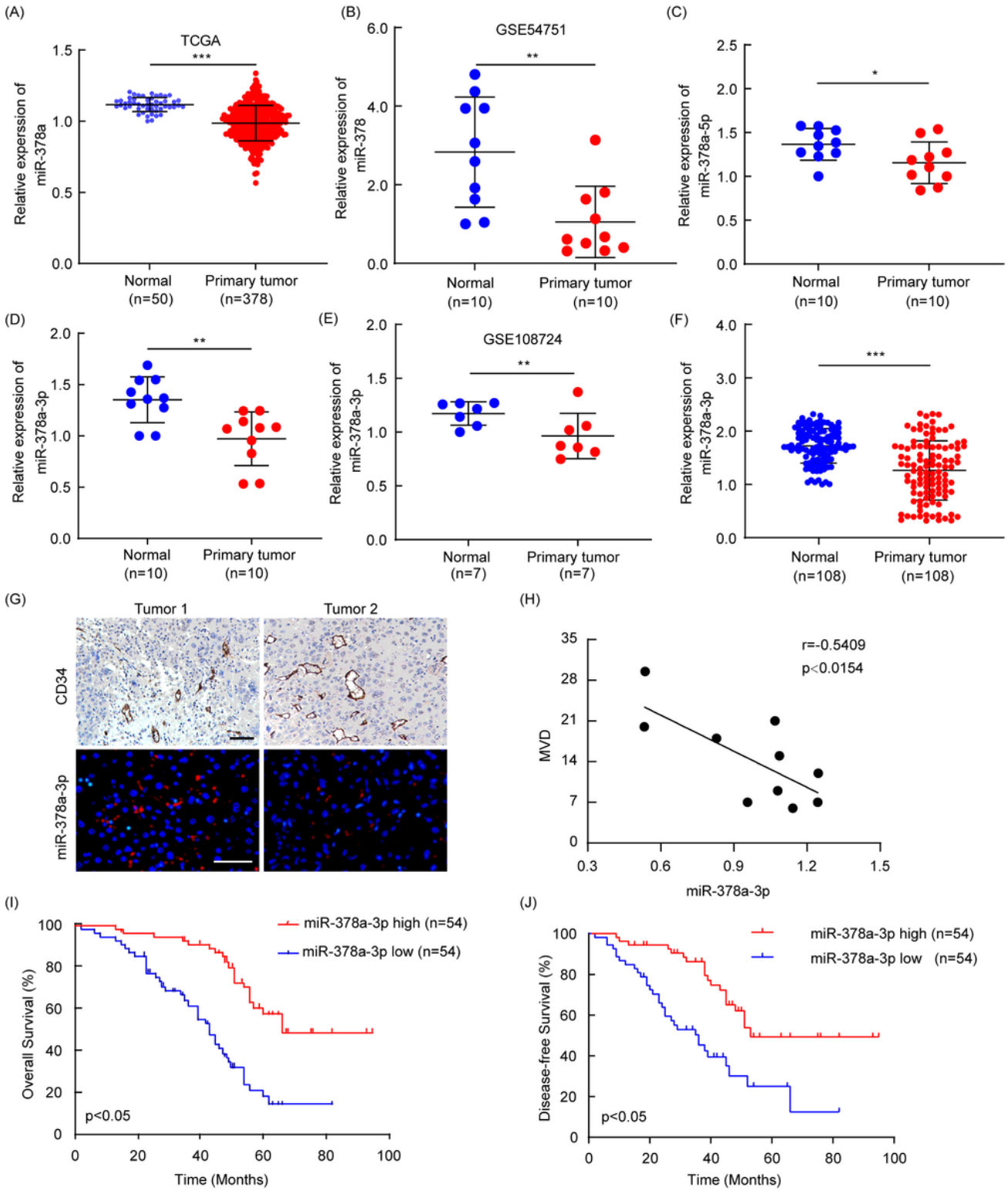

Figure 1

miR-378a-3p expression is downregulated in HCC patients and correlated with HCC angiogenesis. The mRNA expression of miR-378a in HCC and paired normal tissues was analyzed based on TCGA and GEO databases (A, B). Two chains of miR-378a were detected in 10 matched paired normal tissues and HCC tissues by qRT-PCR (C, D). Relative miR-378a-3p mRNA expressions were measured in GEO databases and in 108 pairs of specimens (E, F). Section of tumors were stained with anti-CD34 by IHC and miR-

378a-3p by FISH (G). The correlation line between miR-378a-3p and MVD was analyzed by linear regression analysis (H). OS and DFS was analyzed by high or low expression of miR-378a-3p in patients with HCC by Kaplan–Meier survival curves (I, J). *P < 0.05; **P < 0.01; ***P < 0.001.

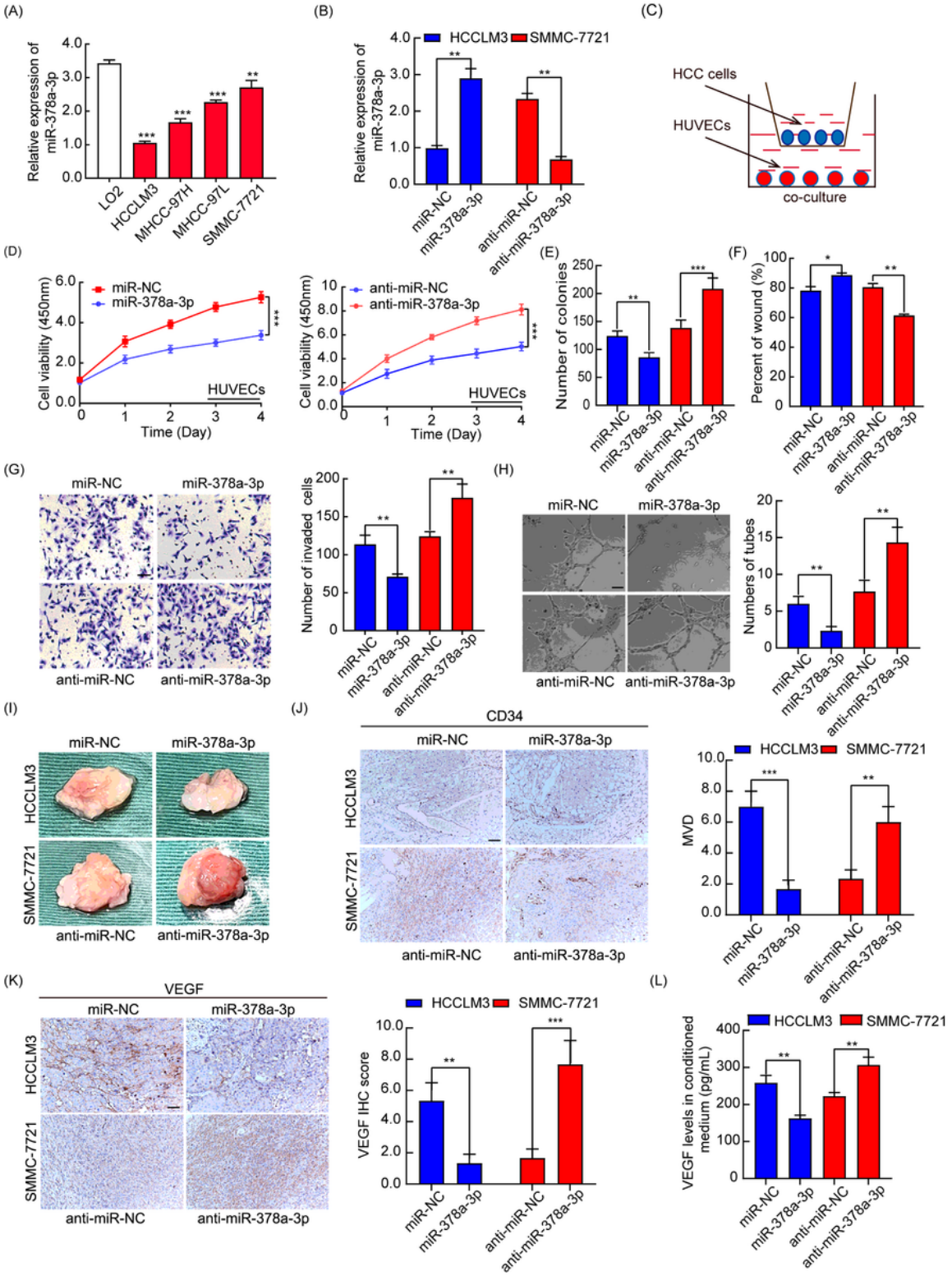

Figure 2

The miR-378a-3p expression inhibited HCC angiogenesis in vitro and in vivo. qRT-PCR analyzed the mRNA expression of miR-378a-3p in different HCC cell lines (A). HCCLM3 and SMMC-7721 cells were

transfected with miR-378a-3p mimic, mimic-NC, inhibitor, or inhibitor-NC, respectively, and analyzed by qRT-PCR (B). A working model of co-culture (C). Treated HUVECs were evaluated by the CCK-8 assay and colony formation assay to analyze cell viability (D, E). Wound healing assay and invasion assays were performed, and the numbers of migration or invasion cells/field were measured (F, G). miR-378a-3p mimic, mimic-NC, inhibitor, or inhibitor-NC RNA were transfected into HCCLM3 and SMMC-7721 cells for 48 h, and then HUVECs tube formation assay was performed and cultured with the conditional supernatant collected from HCC cells (H). Matrigel plugs with treated HCC cells were used to assess the angiogenesis potential (I). Matrigel plugs were collected to perform IHC analysis using the anti-CD34 and anti-VEGF antibody (J, K). The VEGF protein concentration in condition medium of treated HCC cells was detected by ELISA (L). *P < 0.05; **P < 0.01; ***P < 0.001.

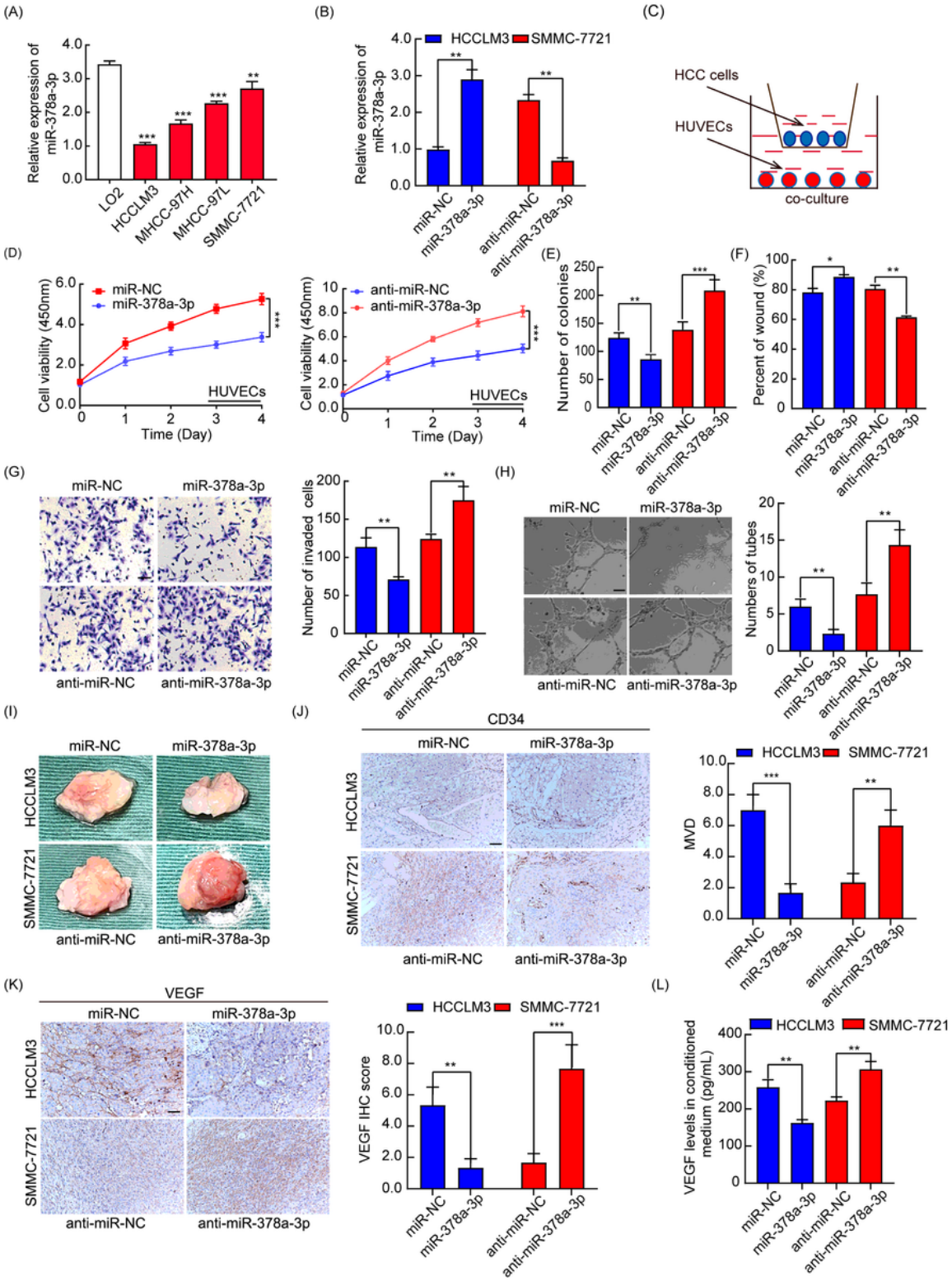

Figure 2

The miR-378a-3p expression inhibited HCC angiogenesis in vitro and in vivo. qRT-PCR analyzed the mRNA expression of miR-378a-3p in different HCC cell lines (A). HCCLM3 and SMMC-7721 cells were transfected with miR-378a-3p mimic, mimic-NC, inhibitor, or inhibitor-NC, respectively, and analyzed by qRT-PCR (B). A working model of co-culture (C). Treated HUVECs were evaluated by the CCK-8 assay and colony formation assay to analyze cell viability (D, E). Wound healing assay and invasion assays were

performed, and the numbers of migration or invasion cells/field were measured (F, G). miR-378a-3p mimic, mimic-NC, inhibitor, or inhibitor-NC RNA were transfected into HCCLM3 and SMMC-7721 cells for 48 h, and then HUVECs tube formation assay was performed and cultured with the conditional supernatant collected from HCC cells (H). Matrigel plugs with treated HCC cells were used to assess the angiogenesis potential (I). Matrigel plugs were collected to perform IHC analysis using the anti-CD34 and anti-VEGF antibody (J, K). The VEGF protein concentration in condition medium of treated HCC cells was detected by ELISA (L). *P < 0.05; **P < 0.01; ***P < 0.001.

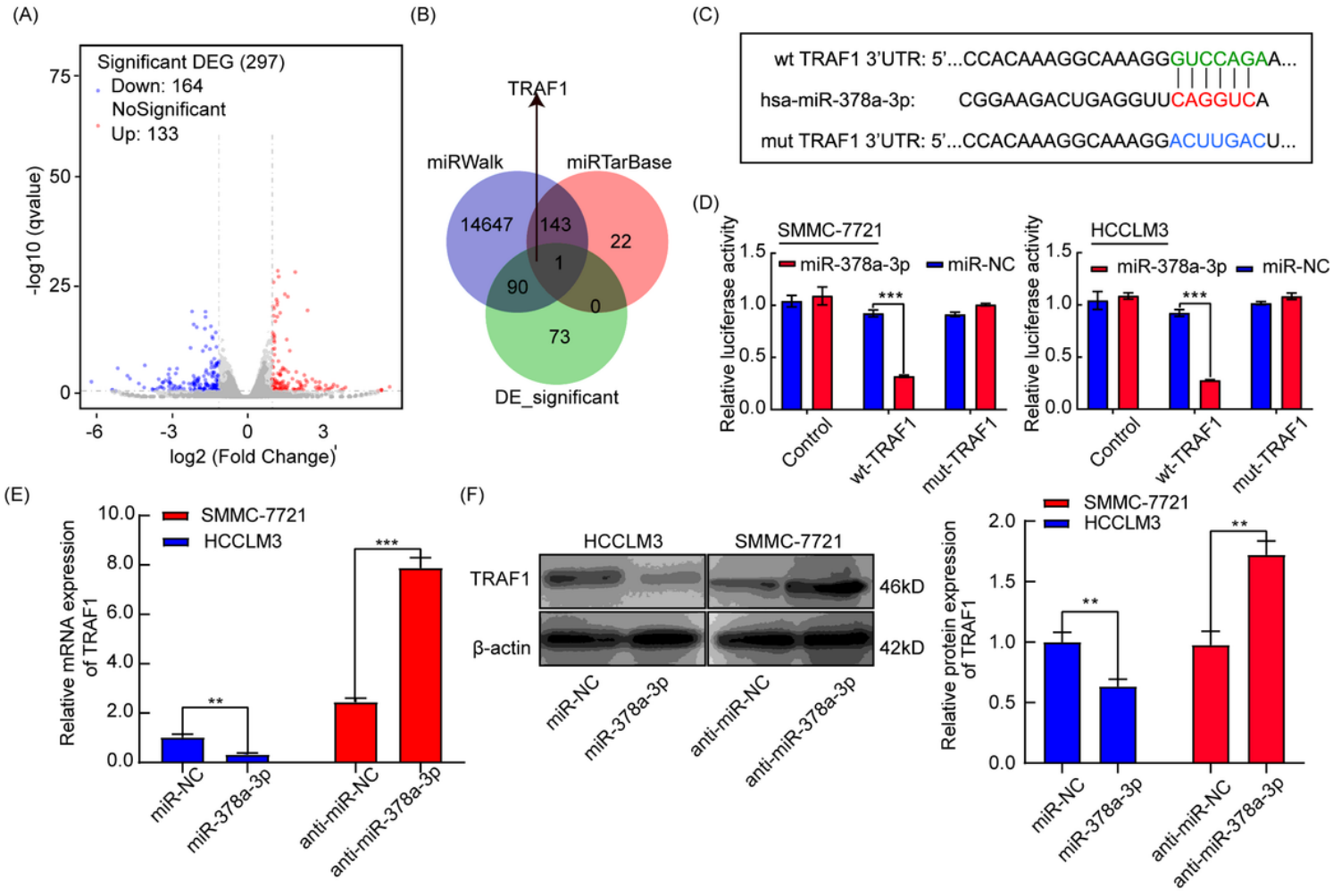

Figure 3

TRAF1 acted as a direct target gene of miR-378a-3p in HCC cells. Three groups of differentially expressed genes between SMMC-7721-overexpression and NC by RNA-seq was performed to find differentially expressed genes (A). Venn diagram of the potential target of miR-378a-3p using two independent algorithms (miRWalk and miRTarBase) combined with our RNA-seq (B). The pattern of TRAF1 3'-UTR wild-type (WT) and mutated type luciferase reporter (C). Relative luciferase activity in SMMC-7721 and HCCLM3 cells co-transfected with miR-378a-3p mimic and TRAF1 (WT) or mutant (MUT) (D). TRAF1 mRNA and protein levels in SMMC-7721 and HCCLM3 cells (E, F). *P < 0.05; **P < 0.01; ***P < 0.001.

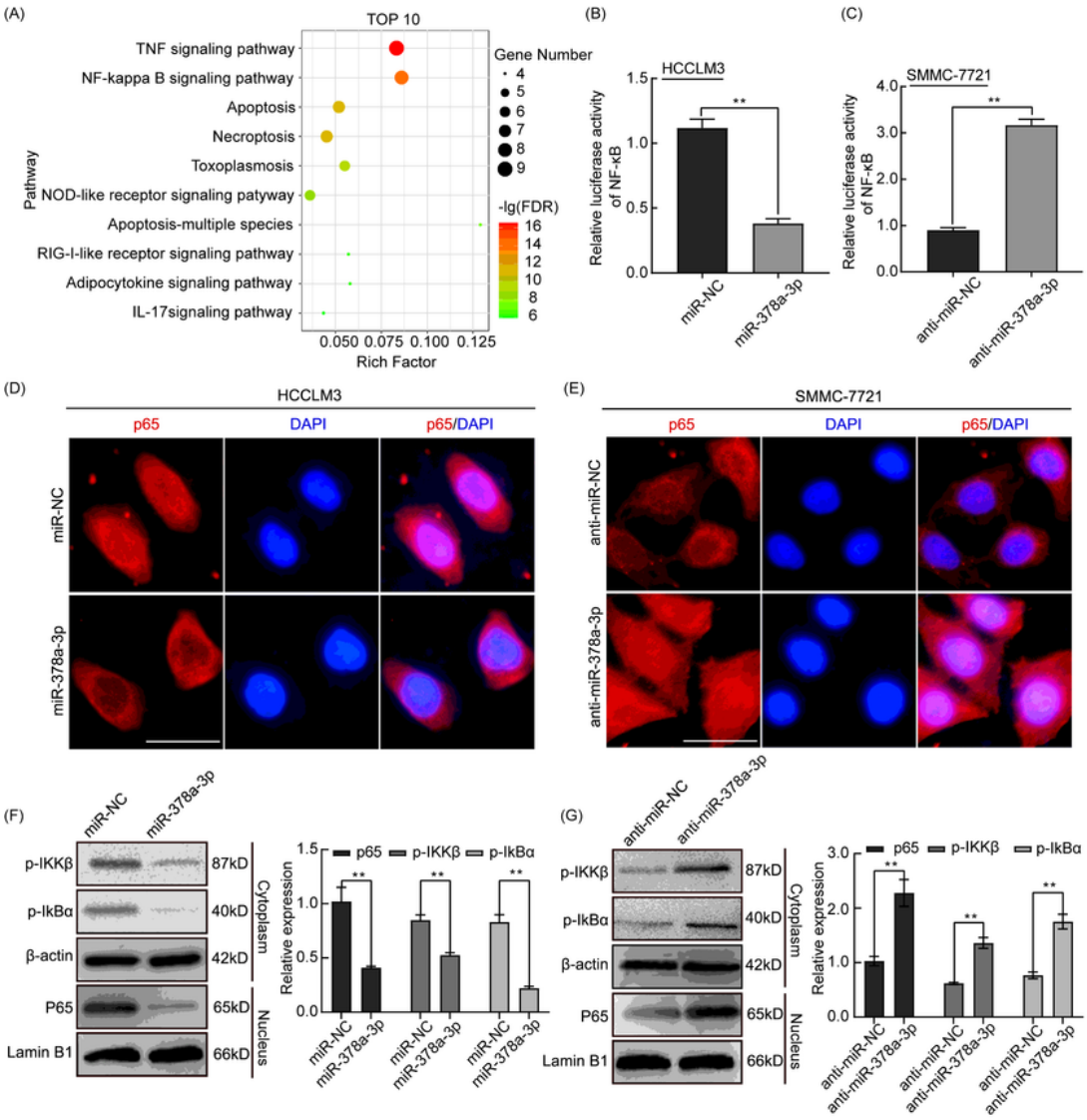

Figure 4

The miR-378a-3p inhibited the activation of the NF-κB signaling pathway by downregulating TRAF1 expression. Signaling pathway enrichment analysis of TRAF1 was analyzed using the online database STRING (A). Relative luciferase activity was detected in SMMC-7721 and HCCLM3 cells transfected with p65 and miR-378a-3p mimic or inhibitor (B, C). Immunofluorescence analysis was done to detect the NF-κB signaling activation in SMMC-7721 and HCCLM3 cells (D, E). The protein expression of NF-κB target

genes transfected with mimic, mimic-NC, inhibitor, or inhibitor-NC RNA was detected by Western blot (F, G). *P < 0.05; **P < 0.01; ***P < 0.001.

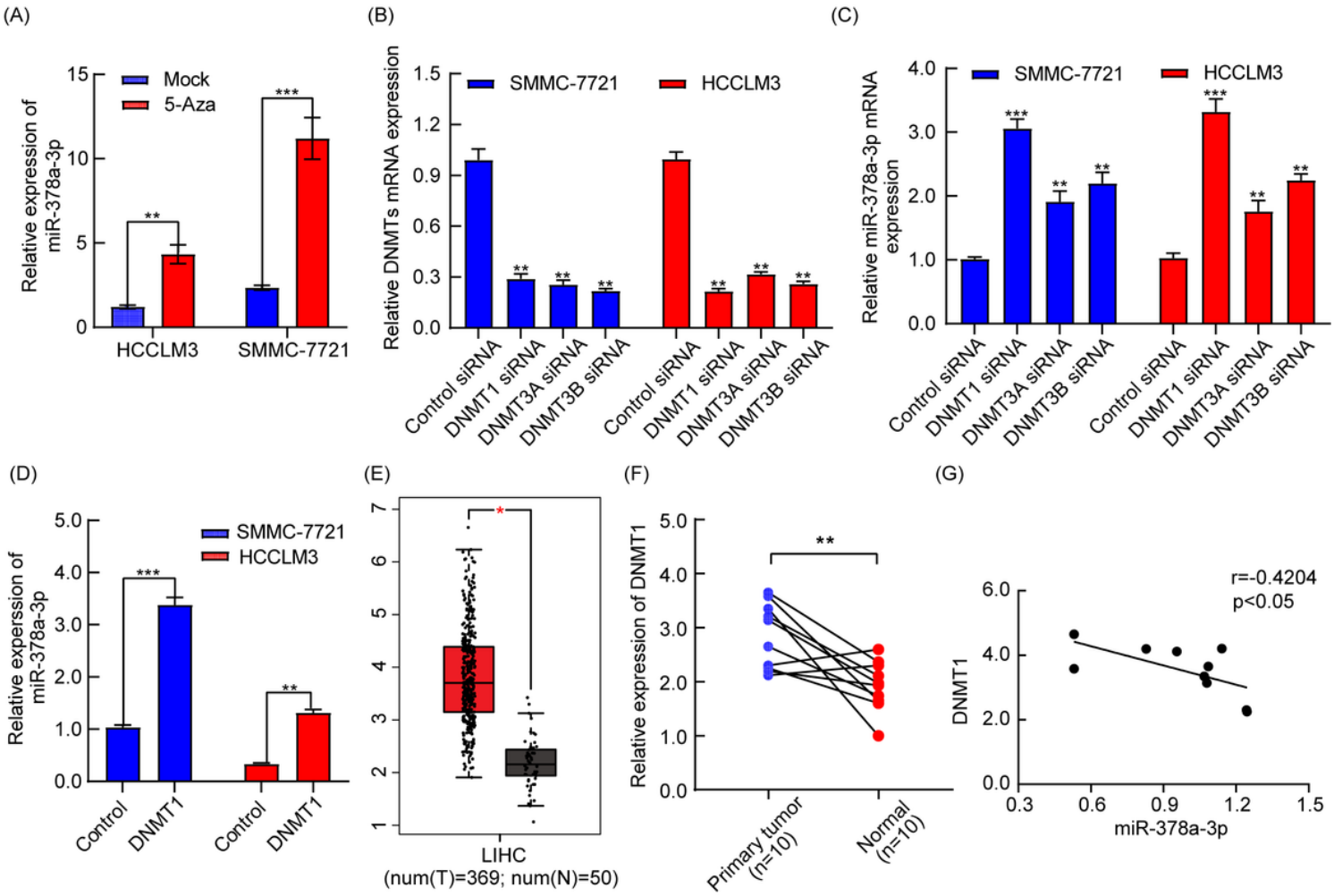

Figure 5

miR-378a-3p is hypermethylated by DNMT1 and silenced in HCC tissues and cells. miR-378a-3p mRNA expression was detected in HCCLM3 and SMMC-7721 cells treated with 10 μM 5-Aza-dC for 48h (A). SMMC-7721 and HCCLM3 cells were transfected with DNMTs siRNA for 48h, DNMTs mRNA expression was measured by qRT-PCR (B). SMMC-7721 and HCCLM3 cells were transfected with DNMTs siRNA for 48h, miR-378a-3p mRNA expression was measured (C). miR-378a-3p mRNA expression was detected in HCC cells transfected with pcDNA-DNMT1 and pcDNA-NC (D). The mRNA expression of DNMT1 in GEPIA database and in 10 paired HCC and adjacent normal tissues was shown (E, F). The relationship between DNMT1 and miR-378a-3p in 10 matched fresh HCC cases was shown (G). *P < 0.05; **P < 0.01; ***P < 0.001.

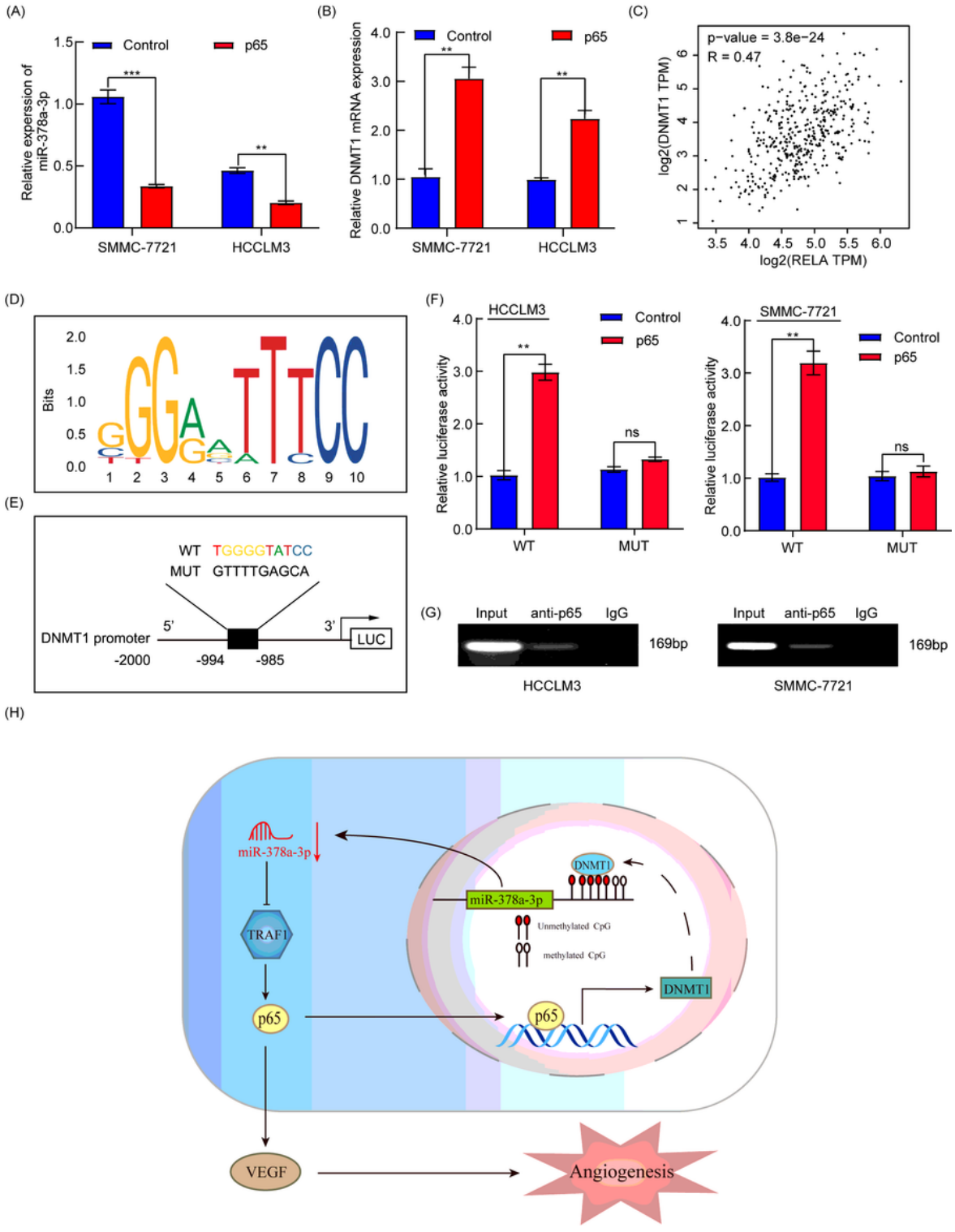

Figure 6

p65 promoted DNMT1 transcription and induced miR-378a-3p silencing mediated by DNA hypermethylation. mRNA expression of miR-378a-3p was detected in different HCC cells transfected with control or p65 (A). The mRNA levels of DNMT1 was detected in HCC cells transfected with control or p65 (B). The relationship between DNMT1 and p65 in the GEPIA database (C). Schematic diagram of binding sites by JASPAR databases (D, E). Detecting the function of p65 on the DNMT1 promoter by luciferase

reporter assays and ChIP assays (F, G). A working model of miR-378a-3p on inhibiting tumor angiogenesis of HCC via inactivating NF-κB signaling pathway (H). *P < 0.05; **P < 0.01; ***P < 0.001.

Supplementary Files

This is a list of supplementary files associated with this preprint. Click to download.

- FigureS1.tif
- FigureS2.tif
- FigureS3.tif
- FigureS4.tif
- TableS1.docx
- TableS2.docx